19th Australasian Fluid Mechanics Conference
Melbourne, Australia
8-11 December 2014

Optical Emission Tomography of Non-axisymmetric, Laminar, Premixed Flames

S. M. Wiseman, A. Haghiri, M. J. Brear, R. L. Gordon, and I. Marusic

Department of Mechanical Engineering
University of Melbourne, VIC 3010, Australia

Abstract

Optical emission tomography of flames has recently been demonstrated as a practical experimental technique for determining the instantaneous position of a 3D flame surface. In this paper, optical emission tomography is applied to steady and forced, non-axisymmetric, premixed, laminar flames. An experimental set-up involving a single camera and a rotatable flame holder allows camera images from an arbitrary number of directions to be obtained. The 3D flame surface is identified and the spatial and temporal resolution of the results is discussed. The dependence of the reconstruction on the number of views is investigated.

Introduction

Unlike conventional point and planar measurement techniques, tomographic methods allow the instantaneous measurement of three-dimensional distributions of a property. It therefore provides unique opportunities in the study of transient 3D flame behaviours [5].

The application of tomographic methods has traditionally been limited by the difficulties and cost associated with obtaining projection measurements, as well as the computational expense of reconstruction algorithms. However, as the cost of both measurement equipment and computational resources continues to decrease, and reconstruction algorithms are optimized for combustion applications, tomographic methods are anticipated to have greater applicability in both combustion research and for on-line diagnostics of industry combustors.

Computerized tomography is the reconstruction of an unknown scalar function f from a finite number of projections and has wide applicability in the fields of science, engineering and medicine [8]. In the terminology of applied tomography, a projection is an integral of a scalar function over a known geometry, which may be a line, area, or volume. A view is a set of projections onto a plane at a defined orientation to the object.

There have been few applications of optical flame tomography in combustion research to date, although there have been several demonstrations of the capabilities of the technique in the literature. Hertz and Faris [9] appear to be the first to apply emission tomography to flames. They reconstructed the CH radical emission intensity profile on a horizontal slice of a laminar, premixed, methane-air flame using 8 views. Ishino and Ohiwa [10] used a custom made 40 lens camera to tomographically reconstruct the emission intensity between 400 - 600 nm of a turbulent premixed flame. Floyd et al. [6, 5] reconstructed the CH radical emission intensity from a laminar matrix burner and a turbulent opposed jet flame. Upton et al. [15] introduced oil droplets into the unburned mixture which burned as they passed through the flame front. Using flash units, Upton et al. reconstructed the scattering intensity to obtain a snapshot of the flame surface geometry.

Reconstruction Algorithms

Reconstruction methods using a finite number of projections can be categorized as either transform methods or series expansion methods [8]. Series expansion methods are commonly preferred for applications where a relatively small number of views are available, as is commonly the case in flame tomography [16]. In series expansion methods a set of J basis functions (b_j) are defined over the reconstruction volume so that f can be approximated by a linear combination of the basis functions [8]:

$$\hat{f} = \sum_{j=1}^{J} x_j b_j, \tag{1}$$

where x_j is the coefficient of basis function b_j, and $\hat{f}$ is a discretization of the scalar function f. The problem of estimating f from its projections can then be expressed as a linear system of equations which can be solved for the coefficients of the basis functions, i.e.

$$y = Rx + e, \tag{2}$$

in which y is a vector containing the projections of f, e is an unknown error vector and R is the weighting matrix. The weighting matrix describes the contribution of each basis function b_j to each projection and can be calculated based on geometry or determined using an image calibration procedure.

The reconstruction region is commonly divided into pixels for 2D reconstructions, or voxels for 3D reconstructions [5, 9, 8]. These basis functions have a value of one inside the element, and zero outside. The coefficient x_j then represents the average value of f over the element. In flame tomography it is commonly assumed that camera images can be treated as orthographic projections of the emission intensity field [10, 6]. For 2D reconstructions the weightings in the matrix R can be determined by calculating the intersection area between a reconstruction pixel and the horizontal area created by projecting a camera pixel through the reconstruction region, after correcting for image magnification.

Many methods exist for calculating a solution to equation 2. Algebraic reconstruction techniques (ART), particularly the multiplicative forms (MART), are perhaps the most widely implemented in the flame tomography literature (e.g. [9, 6, 15]) and are also standard algorithms in tomographic particle image velocimetry [1]. Optimization methods have also been applied in flame tomography, including least squares methods [2], the maximisation of entropy method [7, 3], maximum likelihood estimate methods [10], and total variation minimization [2].

In this paper, a relatively simple and inexpensive experimental setup for optical tomography of steady and forced, non-axisymmetric, laminar flames is presented. The temporal and spatial resolution of flame reconstructions using the MART algorithm is investigated with the aim of clarifying the capabilities and limitations of the technique for combustion research applications. Implications for the study of turbulent flames using optical tomography is also discussed.

Experimental Methods

Tomography of non-axisymmetric flames requires camera images of the object flame from multiple viewing angles. For

steady or periodic, non-axisymmetric flames this can be done with only a single camera. To obtain the desired viewing angles either the camera can be moved around the flame, or the flame orientation can be changed. The arrangement described here uses a rotatable flame holder with a stationary camera. This arrangement naturally is not applicable to turbulent flames.

Laminar Flame Rig

A flame holder with a square port was used to produce steady, non-axisymmetric, laminar, premixed flames. The sides of the port are 22 mm long with rounded corners. The flame holder can be rotated about the vertical axis. A vernier angle scale is used to measure the camera viewing angle to an accuracy of ± 0.1 degrees. A photograph of the rotatable flame holder and vernier scale is shown in figure 1.

Compressed air and propane are mixed approximately three metres upstream of the burner to ensure a well mixed mixture at the burner port [11]. The combustion mixture passes through a 60 mm honeycomb flow straightener in the burner plenum before entering a contraction upstream of the rotatable flame holder. Layers of fine steel mesh before and after the contraction are used to dissipate turbulence. A removable quartz tube protects the flame from surrounding air disturbances and prevents flame flickering caused by buoyancy effects while still allowing optical access.

The flame tip height is extremely sensitive to any change in the flow profile of the unburned mixture and provides a useful indicator of a change in the flame geometry. With the flow conditioning arrangement currently used, the flame tip height varies by less than 0.3 mm as the flame holder is rotated. This is less than the flame thickness and so is unlikely to have significant influence on the reconstruction.

Imaging System

A LaVision Flowmaster 3S camera system, controlled by DaVis 6.2 software, was used to image the flame. The camera is equipped with a 105 mm focal length UV-Nikkor lens, f# 4.5, and a LaVision high-speed IRO image intensifier. For a steady flame, the exposure time can be increased to maximise the signal to noise ratio and the intensifier is not required. The 12 bit camera has a resolution of 1280×1024 and a maximum frame rate of 8 frames per second. The camera was positioned so that the image plane was parallel to the burner centre axis. The sides of the flame holder were used to determine the image magnification and position of the centre of the camera image relative to the centre of the burner.

Coplanar views, such as the views that result from this arrangement, are generally not considered optimal [2]. However, it is one of the simplest tomography arrangements and conveniently allows horizontal slices of the emission intensity field to be reconstructed without reconstructing the emission intensity of the

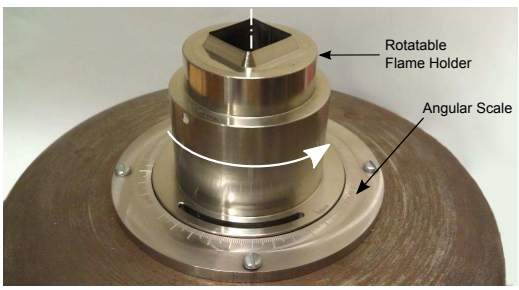

Figure 1: Rotatable flame holder with square port and vernier angle scale for accurate positioning.

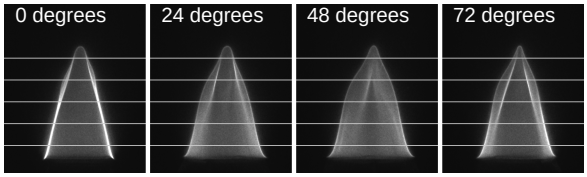

Figure 3: Camera images of a steady, laminar, premixed flame from four viewing angles.

entire flame. Four examples of projection images are included in figure 3. Although no optical filters have been used, some filtering of the flame's emission spectrum is applied by the wavelength dependent properties of components of the imaging system.

Periodically Forced Flame

An 8" speaker bolted to the bottom of the burner plenum is used to excite the flame. A signal generator is connected to the speaker via an audio amplifier, allowing the frequency and amplitude of the acoustic excitation to be controlled. The speaker induces sinusoidal velocity variations in the flow, causing periodic motion of the flame. The voltage output of the signal generator is acquired at 50 kHz by a LabVIEW system and allows the phase of the forcing cycle to be determined when the image intensifier is triggered.

For non-steady flames, the exposure time should ideally be chosen so that the flame moves a distance much smaller than the flame thickness during exposure, to prevent apparent thickening of the flame. The laminar flame speed of propane-air flames at near stoichiometric conditions is around 0.4 m/s. Because the flame typically propagates in the opposite direction to the flow velocity, the flame surface velocity relative to the laboratory is often much less than this. An exception occurs when a pocket of unburned mixture, surrounded by flame, is 'pinched' from the main flame surface. A complicated, non-steady flow field is necessary to produce the mutual flame surface annihilation that results in a separated pocket, and the phenomena is complicated further by the effects of curvature and strain rate on the flame propagation speed. For the flames presented here, it is considered unlikely that the flame velocity relative to the laboratory exceeds 1.5 m/s in most locations. The signal to noise ratio of the camera provides a lower limit on the exposure time. An exposure time of 300 μs was used for the results presented here, limiting the movement of a flame element traveling at 1.5 ms^{-1} to less than 0.45 mm.

Tomographic Reconstruction Algorithm

A 2D implementation of the MART reconstruction algorithm with pixel basis functions [4] was implemented in MATLAB. Due to the experimental arrangement, individual horizontal slices are able to be reconstructed. In practice this corresponds to using the projection measurements from the same row of camera pixels for each viewing angle to reconstruct the intensity field on that plane. A 3D representation of the emission intensity field was obtained by stacking the reconstructed slices.

To calculate the weightings, camera images are treated as orthographic projections of the flame. A common simplification has been implemented where reconstruction pixels are treated as circles with an equal area [1]. The weighting is then independent of the angle of intersections and is only dependent on the shortest distance between a line projected from the centre of the camera pixel and the centre of the reconstruction pixel.

Five iterations of the MART algorithm with a relaxation factor of 0.3 were used to reconstruct the emission intensity field on a 500×500 grid, with a reconstruction pixel length of 0.06 mm.

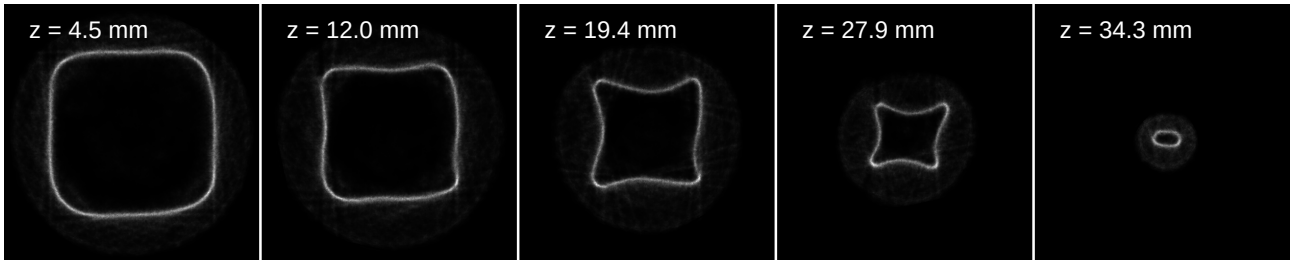

Figure 2: Reconstructed emission intensity in planes perpendicular to the burner axis. The height of each plane above the flame holder is indicated.

There are several possible sources of error introduced by treating the camera images as orthographic projections. These include the camera noise floor, potential non-linearity of the camera intensity response, perception distortion inherent in image formation, and refraction and reflection due to the quartz tube. Additionally, there is uncertainty in the alignment of the camera and flame holder and small variations in the flame during the image acquisition period.

Results and Discussion

Steady Flame

Reconstructions of the emission intensity field on slices through a steady, propane-air flame at near stoichiometric conditions are displayed in figure 2. Thirty views (camera images), equally spaced through 180 degrees, were used to produce the slices. The shape of the flame surface is clearly recognizable and the region of high emission intensity consistently appears to be approximately 8-10 pixels across, corresponding to roughly 0.5-0.6 mm.

Despite relatively good reconstruction of the general flame geometry, reconstruction artefacts are visible upon close inspection. Within the flame, the emission intensity varies in a non-smooth manner and there is little consistency in the emission intensity profile across the flame at different positions on the flame surface. Smoother basis functions, not implemented in the results presented here, may improve the reconstruction. Other features also likely to be reconstruction artefacts include high emission intensities observed in some of the high curvature areas and blurred thickening of the flame. Virtual flame studies may provide some insight into the origin of some of these artefacts.

From the stacked 2D slices, projection images can be calculated from any viewing orientation. A calculated projection image looking down at the flame is provided in figure 4.

Projection images are difficult to interpret due to the superposition of the emission from flame elements along a line of sight. Figure 4 shows rendered partially transparent isosurfaces of the emission intensity field, next to a projection image of the same flame viewed from the same direction. To calculate smooth isosurfaces useful for visualisation purposes, the reconstruction data was smoothed using mean filtering with a $11 \times 11 \times 11$ convolution kernel.

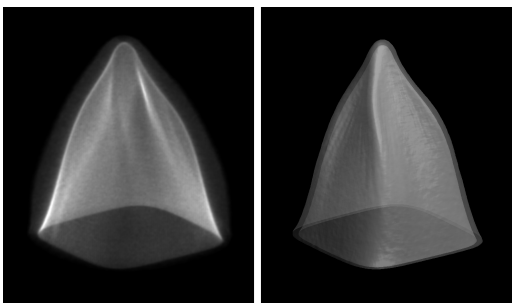

Figure 4: Two visualisations of the same reconstructed emission intensity field from the same viewing angle. Left: calculated projection image; right: rendering of partially transparent isosurfaces of emission intensity.

Periodically Forced Flame

The same tomographic and visualization techniques have been applied to instants in the cycle of a flame forced at 65.7 Hz. Projection images were taken from 18 viewing angles, equally spaced through 180 degrees. Figure 5 shows four sequential instants, each separated by approximately 10 degrees of the forcing cycle, corresponding to an interval of 420 μs between images.

In figure 5 a flame neck pinch-off event is observed, followed by the combustion of a small, separated pocket of unburned mixture [12, 13, 14]. A small detached region of high emission intensity above the tip of the flame can be seen in the third image, showing the final stage of an island burn-out event. Given that the camera exposure time is greater than 70% of the time interval between the images in figure 5, it is clear that there are significant changes in the emission intensity field near mutual flame interaction events during the camera exposure. The reconstructions cannot therefore be treated as accurate snapshots of the emission intensity and a shorter exposure time, likely less than 100 μs is required to investigate such events in detail.

Effect of Number of Views

The accuracy of tomographic reconstruction is known to be highly dependent on the number of views available [8]. Figure 6 shows a reconstructed slice of the steady flame from figure 3 using different numbers of equally spaced views. The number of MART iterations was increased to ten to ensure reasonable convergence of reconstructions that use a small number of views.

Using the current experimental set-up and reconstruction algorithm, more than six views are required to obtain a reasonable estimate of the flame shape. This is consistent with synthetic data studies and other experimental data in the literature. Our experience has shown that for meaningful analysis of the reconstructed emission intensity field, at least 12 views are required.

Conclusions

It has been demonstrated that high resolution tomographic reconstruction of non-axisymmetric, steady or periodic, premixed flames can be performed with a single camera and a relatively simple experimental setup. This requires only a single camera registration procedure. The resulting scalar volume data can be rendered to provide visualisations of the flame at an instant, and to visualise motion of the flame surface. Further post-processing options are also likely to be of interest to the combustion research community, including the calculation of flame thickness, curvature, and flame velocity relative to the laboratory reference frame.

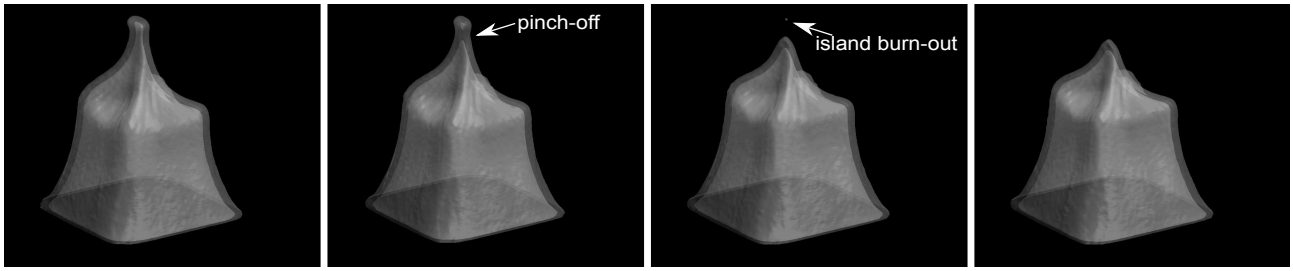

Figure 5: Four sequential instants of a flame forced at 65.7 Hz. There is a time interval of 420 μs between images

With the general MART algorithm and pixel basis functions used in this study, it was found that more than six views of the flame is required to obtain a reasonable representation of the flame geometry. Basis functions or algorithms more suited to reconstructing sparse intensity fields and localised high gradients could yield improved results.

Reconstructions of a forced flame show flame annihilation events occurring in less than 1 ms. This has implications for the tomographic reconstruction of turbulent flames in which such flame interactions may often occur. To capture such events in tomographic reconstructions of turbulent flames requires multiple, high-speed cameras with a frame rate greater than 1000 frames per second.

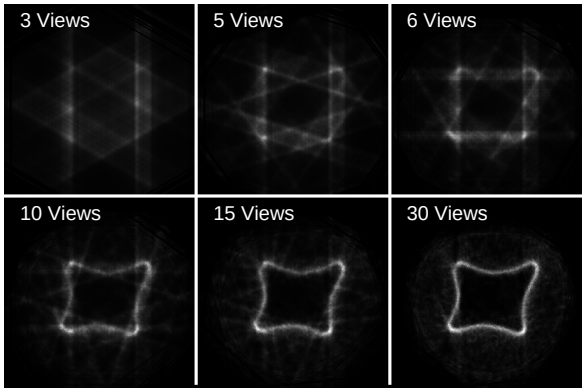

Figure 6: A tomographically reconstructed slice of a steady, premixed flame using different numbers of equally spaced views.

References

[1] Atkinson, C. and Soria, J., An efficient simultaneous reconstruction technique for tomographic particle image velocimetry, *Experiments in Fluids*, **47**, 2009, 553–568.

[2] Cai, W., Li, X., Li, F. and Ma, L., Numerical and experimental validation of a three-dimensional combustion diagnostic based on tomographic chemiluminescence., *Optics Express*, **21**, 2013, 7050 – 7064.

[3] Denisova, N., Tretyakov, P. and Tupikin, A., Emission tomography in flame diagnostics, *Combustion and Flame*, **160**, 2013, 577 – 588.

[4] Elsinga, G. E., *Tomographic particle image velocimetry and its application to turbulent boundary layers*, Ph.D. thesis, Delft University of Technology, 2008.

[5] Floyd, J., Geipel, P. and Kempf, A., Computed tomography of chemiluminescence (ctc): Instantaneous 3d measurements and phantom studies of a turbulent opposed jet flame, *Combustion and Flame*, **158**, 2011, 376 – 391.

[6] Floyd, J. and Kempf, A., Computed tomography of chemiluminescence (ctc): High resolution and instantaneous 3-d measurements of a matrix burner, *Proceedings of the Combustion Institute*, **33**, 2011, 751 – 758.

[7] Goyal, A., Chaudhry, S. and Subbarao, P., Direct three dimensional tomography of flames using maximization of entropy technique, *Combustion and Flame*, **161**, 2014, 173 – 183.

[8] Herman, G. T., *Fundamentals of computerized tomography: image reconstruction from projections*, New York, Springer, 2009.

[9] Hertz, H. M. and Faris, G. W., Emission tomography of flame radicals, *Optics Letters*, **13**, 1988, 351–353.

[10] Ishino, Y. and Ohiwa, N., Three-dimensional computerized tomographic reconstruction of instantaneous distribution of chemiluminescence of a turbulent premixed flame., *JSME International Journal Series B*, **48**, 2005, 34 – 40.

[11] Karimi, N., Brear, M. J., Jin, S.-H. and Monty, J. P., Linear and non-linear forced response of a conical, ducted, laminar premixed flame, *Combustion and Flame*, **156**, 2009, 2201 – 2212.

[12] Talei, M., Brear, M. J. and Hawkes, E. R., Sound generation by laminar premixed flame annihilation, *Journal of Fluid Mechanics*, **679**, 2011, 194–218.

[13] Talei, M., Brear, M. J. and Hawkes, E. R., A parametric study of sound generation by premixed laminar flame annihilation, *Combustion and Flame*, **159**, 2012, 757 – 769.

[14] Talei, M., Hawkes, E. R. and Brear, M. J., A direct numerical simulation study of frequency and lewis number effects on sound generation by two-dimensional forced laminar premixed flames, *Proceedings of the Combustion Institute*, **34**, 2012, 1093–1100.

[15] Upton, T., Verhoeven, D. and Hudgins, D., High-resolution computed tomography of a turbulent reacting flow, *Experiments in Fluids*, **50**, 2011, 125–134.

[16] Verhoeven, D., Limited-data computed tomography algorithms for the physical sciences, *Applied Optics*, **32**, 1993, 3736–3754.